A large eddy simulation approach of compressible turbulent flow without density weighting

Xiao-Bo Sun and Xi-Yun Lu[a]
Department of Modern Mechanics, University of Science and Technology of China,
Hefei, Anhui 230026, China

A large eddy simulation (LES) approach of compressible turbulent flow without density weighting (or Favre averaging) is proposed and examined based on compressible turbulent channel flow. In this Brief Communication, we attempt to remove an inconsistent treatment including both the resolved and Favre-averaged variables and to provide a possible approach to deal with the flows with rapid property variation. The subgrid-scale (SGS) terms in the resolved equations of mass, momentum, and energy conservation are modeled reasonably and the relevant coefficients in the SGS models are computed dynamically. The present LES approach is verified to be reliable and effective by comparing with direct numerical simulation results of compressible turbulent channel flow. © 2006 American Institute of Physics. [DOI: 10.1063/1.2391839]

Large eddy simulation (LES) method has become an efficient tool for the prediction of complex turbulent flows. In LES and Reynolds-averaged Navier-Stokes (RANS) for simulating compressible turbulent flow, it is convenient to use density weighting (or Favre averaging) to simplify the treatments. However, the density weighting may have an intrinsic drawback in predicting the flows with rapid property variation, such as supercritical fluid flow, high Mach number flow, flame stabilization, and shock/boundary layer.[1] To our knowledge, only Boersma and Lele first applied a LES method without density weighting to deal with compressible turbulent jets.[2] Thus, it is highly desirable to develop the relevant method without density weighting.

In LES, to separate the large from the small scales, a filtering operation is introduced and usually defined as

$$\bar{f}(\mathbf{x}) = \int f(\mathbf{x}')G(\mathbf{x},\mathbf{x}';\bar{\Delta})d\mathbf{x}', \tag{1}$$

where an overbar is a filtered or resolved quantity, G is the filter function, and $\bar{\Delta}$ is the filter width. The most commonly used filter functions are the sharp Fourier cutoff, the Gaussian, and the tophat filter. Usually, the LES equations are solved in physical space based on some numerical methods, e.g., finite-difference and finite-volume method, and the corresponding filtered fields are obtained using a tophat filter for its simplicity.[3,4] Here, we employ the tophat filter to deal with the LES equations and the relevant subgrid-scale (SGS) terms. Since the tophat filter is identical with the Reynolds-averaging operator in physical space, we thus can simplify the treatments of the LES equations and the SGS terms.

Applying the filtering operation (1) without density weighting to the equations of mass, momentum and energy conservation, the filtered equations have the following forms:

$$\frac{\partial \bar{\rho}}{\partial t} + \frac{\partial (\bar{\rho}\bar{u}_j)}{\partial x_j} = -\frac{\partial M_j}{\partial x_j}, \tag{2}$$

$$\frac{\partial (\bar{\rho}\bar{u}_i)}{\partial t} + \frac{\partial [\bar{\rho}\bar{u}_i\bar{u}_j + (\gamma-1)C_v\bar{\rho}\bar{T}\delta_{ij} - \bar{\sigma}_{ij}]}{\partial x_j}$$
$$= -\frac{\partial [\tau_{ij} + (\gamma-1)C_v H\delta_{ij}]}{\partial x_j} - \frac{\partial M_i}{\partial t}, \tag{3}$$

$$\frac{\partial \bar{E}}{\partial t} + \frac{\partial \{[\bar{E} + (\gamma-1)C_v\bar{\rho}\bar{T}]\bar{u}_j + \bar{q}_j - \bar{\sigma}_{ij}\bar{u}_i\}}{\partial x_j}$$
$$= -\frac{\partial [\gamma C_v Q_j + \frac{1}{2}J_j - D_j]}{\partial x_j} - \frac{\partial (C_v H + \frac{1}{2}\tau_{kk})}{\partial t}, \tag{4}$$

where u_j is the velocity in the x_j direction, ρ is the density, T is the temperature, C_v is the constant-volume specific heat, C_p is the constant-pressure specific heat, $\gamma = C_p/C_v$ is the ratio of specific heat, and $E = C_v\rho T + 1/2\rho u_k u_k$ is the total energy. It is assumed that $\overline{\mu(T)S_{ij}} \simeq \mu(\bar{T})\bar{S}_{ij}$. Then, the viscous and diffusive fluxes are given by

$$\bar{\sigma}_{ij} = 2\bar{\mu}\bar{S}_{ij} - \frac{2}{3}\bar{\mu}\bar{S}_{kk}\delta_{ij}, \tag{5}$$

$$\bar{q}_j = -\bar{k}\frac{\partial \bar{T}}{\partial x_j}, \tag{6}$$

where $\bar{S}_{ij} = 1/2(\partial \bar{u}_i/\partial x_j + \partial \bar{u}_j/\partial x_i)$ is the strain rate tensor, and $\bar{\mu}$ and $\bar{k}$ are the viscosity and thermal conductivity corresponding to the filtered temperature $\bar{T}$.

These SGS terms, including SGS mass flux M_j, SGS stresses τ_{ij}, SGS heat flux Q_j, SGS density and temperature correlation term H, SGS turbulent diffusion $\partial J_j/\partial x_j$, and SGS viscous diffusion $\partial D_j/\partial x_j$, occur in the filtered equations and are described as

$$M_j = \overline{\rho u_j} - \bar{\rho}\bar{u}_j = \overline{\rho' u_j'}, \tag{7}$$

[a]Author to whom correspondence should be addressed. Electronic mail: xlu@ustc.edu.cn

$$\tau_{ij} = \overline{\rho u_i u_j} - \overline{\rho} \overline{u}_i \overline{u}_j \approx \overline{\rho} \overline{u_i' u_j'} + \overline{u}_i \overline{\rho' u_j'} + \overline{u}_j \overline{\rho' u_i'}, \tag{8}$$

$$Q_j = \overline{\rho T u_j} - \overline{\rho} \overline{T} \overline{u}_j \approx \overline{\rho} \overline{T' u_j'} + \overline{T} \overline{\rho' u_j'} + \overline{u}_j \overline{\rho' T'}, \tag{9}$$

$$H = \overline{\rho T} - \overline{\rho} \overline{T} = \overline{\rho' T'}, \tag{10}$$

$$J_j = \overline{\rho u_j u_k u_k} - \overline{\rho} \overline{u}_j \overline{u}_k \overline{u}_k$$
$$\approx \overline{u}_k \tau_{jk} + \overline{\rho} \overline{u}_j \overline{u_k' u_k'} + \overline{\rho} \overline{u}_k \overline{u_j' u_k'} + \overline{u}_j \overline{u}_k \overline{\rho' u_k'}, \tag{11}$$

$$D_j = \overline{\sigma_{ij} u_i} - \overline{\sigma}_{ij} \overline{u}_i. \tag{12}$$

Here, the approximations by ignoring high-order correlation terms in Eqs. (8), (9), and (11) will be verified to be reliable based on our DNS data below. *A priori* tests using DNS data also confirmed that neglecting the nonlinearities of the diffusion terms in the momentum and energy equations is acceptable.[5]

The SGS terms $\overline{\rho' u_j'}$, $\overline{u_i' u_j'}$, $\overline{T' u_j'}$, and $\overline{\rho' T'}$ in Eqs. (7)–(11) are needed to be modeled and are proposed, respectively. Based on the Boussinesq hypothesis, the SGS mass flux is modeled by

$$\overline{\rho' u_j'} = -C_\rho \bar{\Delta}^2 |\bar{S}| \frac{\partial \bar{\rho}}{\partial x_j}, \tag{13}$$

where $|\bar{S}| = (2\bar{S}_{ij} \bar{S}_{ij})^{1/2}$, and C_ρ is the model coefficient which varies with time and location. The model coefficient C_ρ can be determined by the dynamic procedure.[6,7] After introducing a test filtering with a filter width twice the grid filter width, i.e., $\hat{\bar{\Delta}} = 2\bar{\Delta}$, to the governing equations, the model coefficient can be obtained by

$$C_\rho = \frac{\langle N_j R_j \rangle}{\langle R_k R_k \rangle}, \tag{14}$$

where $N_j = \widehat{\overline{\rho} \overline{u}_j} - \hat{\bar{\rho}} \hat{\bar{u}}_j$, $R_k = \widehat{\mathcal{R}_k} - \hat{\bar{\Delta}}^2 |\hat{\bar{S}}| \partial \hat{\bar{\rho}} / \partial x_k$, $\mathcal{R}_k = \bar{\Delta}^2 |\bar{S}| \times \partial \bar{\rho} / \partial x_k$, the symbol $\wedge$ represents a test filtered quantity, and $\langle \rangle$ denotes some kind of spatial averaging to remove the calculation oscillation.[6,7]

To model the SGS term $\overline{u_i' u_j'}$, an eddy-viscosity subgrid-scale model was used and represented as[8]

$$\overline{u_i' u_j'} - \frac{\delta_{ij}}{3} \overline{u_k' u_k'} = -2C_u \bar{\Delta}^2 F \left(\bar{S}_{ij} - \frac{\delta_{ij}}{3} \bar{S}_{kk} \right), \tag{15}$$

where $B_\beta = \beta_{11}\beta_{22} - \beta_{12}^2 + \beta_{11}\beta_{33} - \beta_{13}^2 + \beta_{22}\beta_{33} - \beta_{23}^2$, $\alpha_{ij} = \partial \bar{u}_j / \partial x_i$, $\beta_{ij} = \alpha_{mi}\alpha_{mj}$, and $F = [B_\beta / (\alpha_{ij}\alpha_{ij})]^{1/2}$.

This model is constructed in such a way that its dissipation is relatively small in transitional and near-wall regions, and *a priori* model coefficient C_u is given empirically.[8] Here, the corresponding dynamic model is proposed with the model coefficient,

$$C_u = \frac{\langle L_{ij} A_{ij} \rangle}{\langle A_{lk} A_{lk} \rangle}, \tag{16}$$

where $L_{ij} = \widehat{\overline{u}_i \overline{u}_j} - \hat{\bar{u}}_i \hat{\bar{u}}_j$, $A_{lk} = \widehat{\mathcal{A}_{lk}} - 2\hat{\bar{\Delta}}^2 \hat{F}(\hat{\bar{S}}_{lk} - \hat{\bar{S}}_{mm} \delta_{lk}/3)$, and $\mathcal{A}_{lk} = 2\bar{\Delta}^2 F(\bar{S}_{lk} - \bar{S}_{mm} \delta_{lk}/3)$.

Similarly, the SGS term $\overline{T' u_j'}$ is modeled by

$$\overline{T' u_j'} = -C_T \bar{\Delta}^2 |\bar{S}| \frac{\partial \bar{T}}{\partial x_j}. \tag{17}$$

Then, the model coefficient C_T is obtained by

$$C_T = \frac{\langle K_j B_j \rangle}{\langle B_k B_k \rangle}, \tag{18}$$

where $K_j = \widehat{\overline{T} \overline{u}_j} - \hat{\bar{T}} \hat{\bar{u}}_j$, $B_k = \widehat{\mathcal{B}_k} - \hat{\bar{\Delta}}^2 |\hat{\bar{S}}| \partial \hat{\bar{T}} / \partial x_k$, and $\mathcal{B}_k = \bar{\Delta}^2 |\bar{S}| \times \partial \bar{T} / \partial x_k$.

Based on modified Reynolds analogies which could be applied to an isothermal wall,[9] a relation is used as

$$\frac{T'/\bar{T}}{(\gamma - 1)\bar{M}_a^2 u_1'/\bar{u}_1} \approx C_R, \tag{19}$$

where $\bar{M}_a$ is a local Mach number, C_R is a parameter corresponding to different Reynolds analogies and $C_R = 1/(\partial \bar{T}_t / \partial \bar{T} - 1)$ used here with T_t being a total temperature. Then, $\overline{\rho' T'}$ is expressed as

$$\overline{\rho' T'} = C_R(\gamma - 1)\bar{M}_a^2 \overline{T} \overline{\rho' u_1'} / \bar{u}_1. \tag{20}$$

The SGS viscous diffusion in Eq. (12) is negligibly small in the energy equation based on numerical tests.[10] Thus, we neglect this term without any model. According to our treatment, the pressure can be reliably obtained from the equation of state by the resolved variables and the SGS term, i.e., Eq. (20), involving the compressibility effect and the relevant thermal effect.[4]

To examine the present LES approach, a fully developed compressible turbulent channel flow with isothermal walls is investigated by solving Eqs. (2)–(4). The time integration is performed by an explicit third-order Runge-Kutta scheme. A fourth-order centered finite difference scheme is used for the convective and pressure gradient terms. Diffusive terms and SGS terms are discretized with a second-order centered scheme. To minimize the aliasing error, the nonlinear terms are treated in the skew symmetric form. The code used here has been validated extensively.[11]

The computational domain is $[0, 4\pi H] \times [0, 4\pi H/3] \times [-H, H]$ in the streamwise, spanwise and wall-normal direction, denoted by $x_1(x)$, $x_2(y)$, and $x_3(z)$, respectively, with H the channel half-width. The nondimensional parameters are defined as follows. The Reynolds number, $\text{Re} = \rho_m U_m H / \mu_w$, is based on the bulk density, bulk velocity, channel half-width, and viscosity at the isothermal wall, and the Mach number, $M = U_m / (\gamma R T_w)^{1/2}$ with $R = (\gamma - 1)C_p / \gamma$ being the gas constant, is based on the sound speed at the isothermal wall. The parameters for the present simulation are $\text{Re} = 3000$, $M = 1.5$, $\gamma = 1.4$, and the Prandtl number $\text{Pr} = 0.72$. The viscosity is given by Sutherland's law, i.e., $\bar{\mu} = \bar{T}^{3/2}(1 + S_1/T_w)/(\bar{T} + S_1/T_w)$, where $S_1 = 110.4$ K and $T_w = 293.15$ K.

Mesh characteristics and mean flow variables for our DNS and LES are summarized in Table I. The grids, the same as previous simulations,[12] are uniform in the x_1 and x_2 directions and hyperbolic-tangent stretching distribution in the x_3 direction. The parameters N_1, N_2, and N_3 are the num-

TABLE I. Mesh characteristics and mean flow variables.

	$N_1 \times N_2 \times N_3$	$\min(\Delta x_3^+)$	Re_τ	u_τ	M_c	$C_f \times 10^3$	ρ_w
Present DNS	$192 \times 128 \times 181$	0.35	216	0.0525	1.508	7.55	1.368
Present LES	$96 \times 64 \times 91$	0.74	221	0.0538	1.502	7.92	1.369
Morinishi *et al.* (Ref. 12)	$120 \times 120 \times 180$	0.35	218	0.0533	1.502	7.74	1.362

ber of grid points for each direction and Δx_3^+ is the grid spacing normal to the wall expressed in wall units. Re_τ and u_τ represent the friction Reynolds number and friction velocity. M_c is the mean channel center line Mach number, C_f is skin friction coefficient and ρ_w represents mean density on the isothermal wall. As exhibited in Table I, the present LES and DNS results agree well with the previous DNS data.[12]

To verify the reliability of approximations in Eqs. (8), (9), and (11), *a priori* tests are carried out. By applying the tophat filter to the DNS data, the terms on both the sides of the approximate equal-sign of these equations are calculated. In Eq. (8), it is identified that $\overline{\rho u_i' u_j'}$ is a dominant term. Typically, Figs. 1(a) and 1(b) show the profiles of each term for τ_{11} and τ_{13}. It is confirmed that the SGS stresses τ_{ij} are well approximated by the terms on the right-hand side of Eq. (8) based on the good comparisons between term-1 and term-4 in Fig. 1(a) or term-1 and term-5 in Fig. 1(b). Similarly, Figs. 1(c) and 1(d) show the distributions of each term for Q_3 and J_1, respectively. Good agreements between term-1 and term-5 in Fig. 1(c) or term-1 and term-6 in Fig. 1(d) suggest that the approximate treatments in Eqs. (9) and (11) are reliable. In addition, it is noticed that the terms on the right-hand side of Eqs. (9) and (11) are nearly comparable;

an attempt to model only typical term may not be reliable and could bring unsatisfied predictions.[11]

For an assessment of the correlation between modeled and exact data, *a priori* analysis of the DNS database is performed. The variables obtained by our DNS data are filtered to yield the exact SGS terms, which are used to assess the accuracy of the parametrization. Then, the accuracy of the models used above is evaluated by computing the exact SGS term and their modeling term and comparing both the exact and modeling terms using their correlation coefficient.[11] Since the eddy-viscosity type models are used in this study, the correlation coefficients for $\overline{\rho' u_j'}$, $\overline{u_i' u_j'}$, and $\overline{T' u_j'}$ $(i,j=1,2,3)$ are in the range of 0.1–0.3, which are consistent with the predictions.[11] It is needed to indicate that the turbulence statistics calculated by the eddy-viscosity type models may still be reliably predicted compared with the results obtained by other SGS models, e.g., dynamic mixed model, whose correlation coefficients are in the range 0.8–0.9.[5,13]

A priori tests of the model coefficients in the SGS models are carried out. Figure 2(a) shows the distributions of the instantaneous model coefficient C_u calculated by the LES
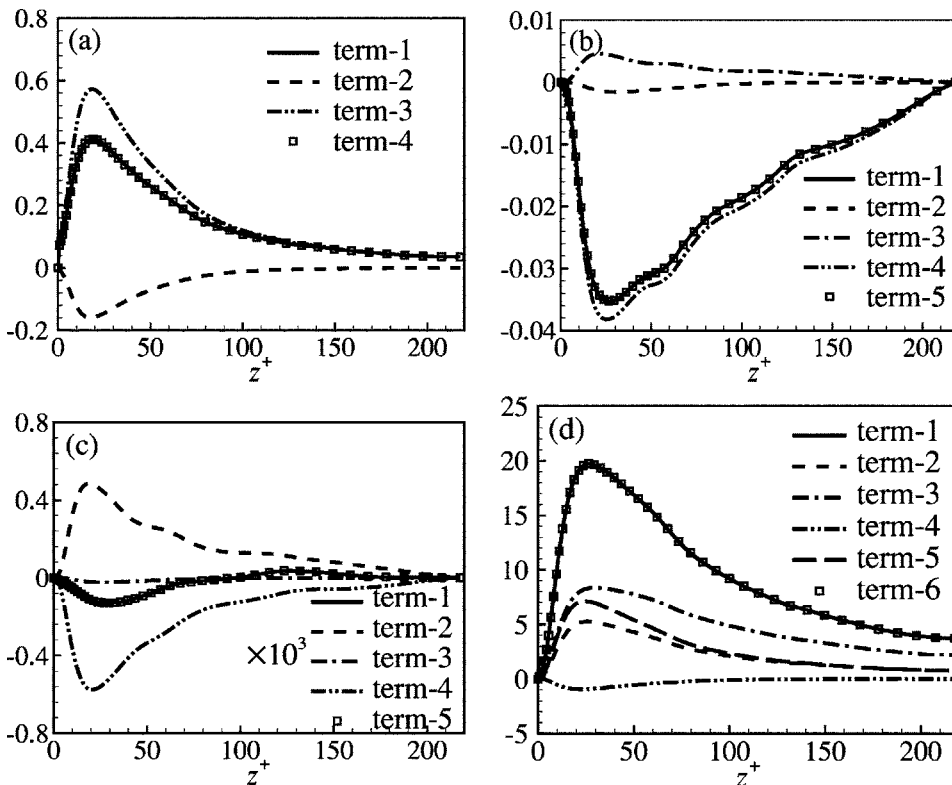
FIG. 1. Profiles of the subterms in the SGS terms. (a) $\langle\tau_{11}\rangle$, normalized by $\rho_w u_\tau^2$, with term-1: $\langle\overline{\rho u_1 u_1}-\overline{\rho}\overline{u}_1^2\rangle$, term-2: $\langle 2\overline{u}_1\overline{\rho' u_1'}\rangle$, term-3: $\langle\overline{\rho u_1' u_1'}\rangle$, and term-4: $\langle 2\overline{u}_1\overline{\rho' u_1'}\rangle+\langle\overline{\rho u_1' u_1'}\rangle$; (b) $\langle\tau_{13}\rangle$, normalized by $\rho_w u_\tau^2$, with term-1: $\langle\overline{\rho u_1 u_3}-\overline{\rho}\overline{u}_1\overline{u}_3\rangle$, term-2: $\langle\overline{u}_3\overline{\rho' u_1'}\rangle$, term-3: $\langle\overline{u}_1\overline{\rho' u_3'}\rangle$, term-4: $\langle\overline{\rho u_1' u_3'}\rangle$, and term-5: $\langle\overline{u}_3\overline{\rho' u_1'}\rangle+\langle\overline{u}_1\overline{\rho' u_3'}\rangle+\langle\overline{\rho u_1' u_3'}\rangle$; (c) $\langle Q_3\rangle$, normalized by $\rho_w u_\tau T_w$ and multiplied by 10^3, with term-1: $\langle\overline{\rho u_3 T}-\overline{\rho}\overline{u}_3\overline{T}\rangle$, term-2: $\langle\overline{T}\overline{\rho' u_3'}\rangle$, term-3: $\langle\overline{u}_3\overline{\rho' T'}\rangle$, term-4: $\langle\overline{\rho T' u_3'}\rangle$, and term-5: $\langle\overline{\rho T' u_3'}\rangle+\langle\overline{T}\overline{\rho' u_3'}\rangle+\langle\overline{u}_3\overline{\rho' T'}\rangle$; (d) $\langle J_1\rangle$, normalized by $\rho_w u_\tau^3$, with term-1: $\langle\overline{\rho u_1 u_k u_k}-\overline{\rho}\overline{u}_1\overline{u}_k\overline{u}_k\rangle$, term-2: $\langle\overline{u}_k\tau_{1k}\rangle$, term-3: $\langle\overline{\rho u_1 u_k' u_k'}\rangle$, term-4: $\langle\overline{u}_1\overline{u}_k\overline{\rho' u_k'}\rangle$, term-5: $\langle\overline{\rho}\overline{u}_k\overline{u_1' u_k'}\rangle$, and term-6: $\langle\overline{u}_k\tau_{1k}\rangle+\langle\overline{\rho u_1 u_k' u_k'}\rangle+\langle\overline{\rho}\overline{u}_k\overline{u_1' u_k'}\rangle+\langle\overline{u}_1\overline{u}_k\overline{\rho' u_k'}\rangle$.
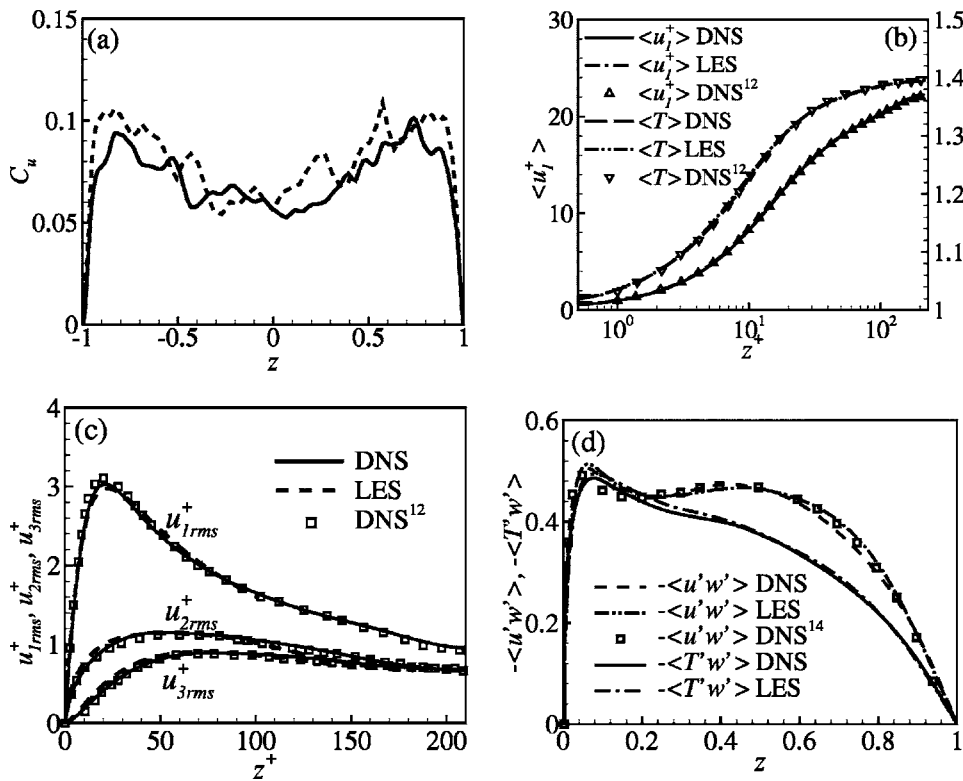
FIG. 2. Comparison of the calculated results: (a) model coefficient C_u calculated by Eq. (16) in the LES (dashed line) and based on the filtered DNS data (solid line); (b) mean velocity $\langle u_1^+ \rangle$ and temperature $\langle T \rangle$; (c) turbulent intensities normalized by u_τ; (d) shear stress $-\langle u_1' u_3' \rangle$ normalized by $\langle u_{1\mathrm{rms}} \rangle \times \langle u_{3\mathrm{rms}} \rangle$, and turbulent heat flux $-\langle T' u_3' \rangle$ normalized by $\langle T_{\mathrm{rms}} \rangle \langle u_{3\mathrm{rms}} \rangle$, where rms denotes the root-mean-square value of fluctuation.

and by the filtered DNS data. Both the predicted results agree reasonably with each other. The profiles of C_u damps quickly in the near-wall regions, proving that the dissipation of the eddy-viscosity model is relatively small in the wall regions.[8]

Furthermore, to validate the present LES, the mean velocity and temperature predicted by the LES and DNS agree well over the channel in Fig. 2(b). The velocity fluctuations are shown in Fig. 2(c) to demonstrate that the present LES prediction for turbulent intensities is satisfactory. It is also seen that the present LES and DNS results agree well with previous DNS data.[12] The profiles of the shear stress and turbulent heat flux in Fig. 2(d) obtained by the LES and DNS agree well with each other, and the shear stress is in a good agreement with previous DNS data.[14] Moreover, we have compared other turbulent quantities with the DNS results and can confirm that the present LES is able to predict turbulence characteristics of compressible turbulent flow.

In summary, the LES approach of compressible turbulent flow without density weighting is proposed and the relevant SGS models are reasonably developed to model the SGS terms in the resolved equations of mass, momentum, and energy conservation. The present LES approach is verified to be reliable and effective by comparing DNS results of compressible turbulent channel flow. Although we recognize the limitation of using the channel flow to verify this LES approach, the present effort has provided interesting insights and successful simulations. Our further work will attempt to apply this approach to deal with some flows with rapid property variation.

[1] V. Yang, "Modeling of supercritical vaporization, mixing, and combustion processes in liquid-fueled propulsion systems," Proc. Combust. Inst. **28**, 925 (2000).
[2] B. J. Boersma and S. K. Lele, "Large eddy simulation of compressible turbulent jets," in *Center for Turbulence Research, Annual Research Briefs* (Center for Turbulence Research, Stanford, CA, 1999), p. 365.
[3] S. B. Pope, *Turbulent Flows* (Cambridge University Press, New York, 2000).
[4] X. Y. Lu, S. W. Wang, H. G. Sung, S. Y. Hsieh, and V. Yang, "Large eddy simulations of turbulent swirling flows injected into a dump chamber," J. Fluid Mech. **527**, 171 (2005).
[5] B. Vreman, B. Geurts, and H. Kuerten, "Subgrid-modelling in LES of compressible flow," Appl. Sci. Res. **54**, 191 (1995).
[6] M. Germano, U. Piomelli, P. Moin, and W. Cabot, "A dynamic subgrid-scale eddy viscosity model," Phys. Fluids A **3**, 1760 (1991).
[7] G. Erlebacher, M. Y. Hussaini, C. G. Speziale, and T. A. Zang, "Toward the large-eddy simulation of compressible turbulent flows," J. Fluid Mech. **238**, 155 (1992).
[8] A. W. Vreman, "An eddy-viscosity subgrid-scale model for turbulent shear flow: Algebraic theory and applications," Phys. Fluids **16**, 3670 (2004).
[9] P. G. Huang, G. N. Coleman, and P. Bradshaw, "Compressible turbulent channel flow: DNS results and modelling," J. Fluid Mech. **305**, 185 (1995).
[10] M. P. Martin, U. Piomelli, and G. V. Candler, "Subgrid-scale models for compressible large-eddy simulations," Theor. Comput. Fluid Dyn. **13**, 361 (2000).
[11] E. Lenormand, P. Sagaut, L. Ta Phuoc, and P. Comte, "Subgrid-scale models for large-eddy simulation of compressible wall bounded flows," AIAA J. **38**, 1340 (2000).
[12] Y. Morinishi, S. Tamano, and K. Nakabayashi, "Direct numerical simulation of compressible turbulent channel flow between adiabatic and isothermal walls," J. Fluid Mech. **502**, 273 (2004).
[13] F. Sarghini, U. Piomelli, and E. Balaras, "Scale-similar models for large-eddy simulations," Phys. Fluids **11**, 1596 (1999).
[14] G. N. Coleman, J. Kim, and R. D. Moser, "A numerical study of turbulent supersonic isothermal-wall channel flow," J. Fluid Mech. **305**, 159 (1995).